UK Atomic Energy Authority

UKAEA-STEP-CP(24)04

A. Fil, L. Henden, S. Newton, T. Hender, M. Hoppe

Disruption runaway electron generation and mitigation in the Spherical Tokamak for Energy Production

Disruption runaway electron generation and mitigation in the Spherical Tokamak for Energy Production

A. Fil, L. Henden, S. Newton, T. Hender, M. Hoppe

This paper has been submitted to
29th IAEA Fusion Energy Conference (FEC 2023), London, 16-21 October 2023

DISRUPTION RUNAWAY ELECTRON GENERATION AND MITIGATION IN THE SPHERICAL TOKAMAKS FOR ENERGY PRODUCTION

A. FIL, L. HENDEN, S. NEWTON
United Kingdom Atomic Energy Authority, Culham Science Centre
Abingdon, Oxfordshire, United Kingdom
Email: alexandre.fil@ukaea.uk

M. HOPPE
Department of Electrical Engineering, KTH Royal Institute of Technology
Stockholm, Sweden

O. VALLHAGEN
Department of Physics, Chalmers University of Technology
Gothenburg, Sweden

Abstract

Generation of Runaway Electrons (REs) during plasma disruptions, and their impact on plasma facing components, is of great concern for ITER and future reactors based on the tokamak concept, such as STEP (Spherical Tokamak for Energy Production). The STEP concept design flat top operating point features a plasma current higher than 20 MA and thus any STEP plasma disruption is expected to be in the seed-insensitive regime of avalanche multiplication, i.e., any runaway seed would quickly generate a large runaway beam during the current quench. This is confirmed by modelling runaway electron generation in an unmitigated disruption using the state-of-the-art code DREAM. Hot-tail generation of runaways is found to be the dominant primary generation mechanism, and the avalanche multiplication factor is confirmed to be extremely high. Even by varying assumptions for the prescribed thermal quench phase (duration, final electron temperature) in a reasonable physical range, as well as the wall time, the plasma-wall distance, and shaping effects, we find that all STEP unmitigated disruptions generate runaway electron beams with more than 10 MA of current (up to full conversion).
The possibility of RE avoidance by idealized, i.e. radially uniform, impurity injection of a mixture of argon and D_2 is then modelled, with ad-hoc particle transport arising from the stochasticity of the magnetic field during the thermal quench (TQ). Unfortunately, no such injection scenario allows runaways to be avoided while respecting the other constraints of disruption mitigation: current quench time between 20 and 120 ms, thermal energy radiated fraction above 90%, and heat impact factor (HIF) lower than 60 $MJ.m^2.s^{-0.5}$ to avoid W melting during the mitigated disruption radiation flash.
The current STEP disruption mitigation system (DMS) concept design has then been tested with DREAM, scanning 2-stage Shattered Pellet Injections consisting of pure deuterium pellets followed by mixed pellets of argon and deuterium (12×15 injectors in total). Such a scheme is found to reduce the generation of REs by the hot-tail mechanism, reducing the final RE current to about 12 MA (instead of 15 MA with a single pure argon injection), but isn't sufficient to avoid the generation of a large RE beam, which would need to be mitigated through additional deuterium SPIs or MGIs (30 injectors are planned in STEP, dedicated to that purpose). With the SPI modelling, the range of impurity densities achieved is significantly reduced compared to the idealised impurity injections, and thus the final RE current is rather insensitive to the number of pellets injected (because larger quantities are not ablated and assimilated by the plasma). The results are much more sensitive to the choice of stochastic particle transport during the thermal quench (both amplitude and duration), which should be better constrained by future 3D non-linear MHD modelling of STEP mitigated disruptions.

1. INTRODUCTION

Generation of Runaway Electrons (REs) during plasma disruptions, and their potential impact on the plasma facing components (PFCs), is of great concern for ITER [1] and future reactors based on the tokamak concept. The STEP (Spherical Tokamak for Energy Production) programme [2] aims at producing net energy from a prototype fusion energy plant and at its current flat top operating point, the plasma current is higher than $20\ MA$. It is thus expected to be in the seed-insensitive regime of avalanche multiplication, i.e., any runaway seed would quickly generate a large runaway beam during unmitigated disruption current quenches. Indeed, recent studies on ITER [3], SPARC [4] and a smaller STEP concept [5] have shown that such plasmas are prone to large RE beams during disruptions, even mitigated ones. Several modelling tools have been developed in the past few years to better model the

generation of runaway electrons, including NIMROD [6], M3D-C1 [7], JOREK [8], MARS-F [9], and the code used in this study: DREAM [10]. Most of those codes are 3D non-linear MHD codes, computationally expensive, and more suitable for the modelling of existing experiments or an already well-defined scenario. As STEP is still in the concept design phase, a faster, modular, open-source code such as DREAM was the best option to quickly explore and map the operational space of STEP DMS. DREAM is modular in the sense that it can be run with different models for runaways and the background plasma population, i.e. as in fluid, isotropic or fully kinetic. More details can be found in [5] or [10]. It can be run with prescribed temperature profiles, a feature which will be used to model unmitigated disruptions in section 2, or self-consistent temperature evolution with idealised impurity injection. The latter will be used to explore runaway generation in STEP for varying injected impurity densities in section 3. DREAM also includes a model for SPI, that will be used extensively in section 4 to test STEP DMS concept design. In this paper, we use DREAM in fully fluid mode (as in [5]), the implication of this assumption (and other assumptions of the modelling) will be discussed in section 5.

2. UNMITIGATED DISRUPTIONS

All simulations presented in this paper start from a STEP flat top operating point (STEP-EC-HD-v3) obtained using the integrated modelling tool JETTO [2], which provides DREAM with initial profiles for the plasma density, temperature and parallel current density. Main parameters of STEP-EC-HD-v3 are: $R_0 = 3.6\ m$, $B_{T,0} = 3.2\ T$, $I_p = 20\ MA$, $T_{e,0} = 20\ keV$, $n_{e,0} = 1.4.10^{20}\ m^{-3}$ and total thermal and magnetic energies of $E_{th} = 580\ MJ$ and $E_{mag} = 127\ MJ$. A free-boundary equilibrium file is also provided by the code FIESTA, from which Miller parameters (i.e. triangularity, elongation, Shafranov shift, etc) are extracted, either using DREAM tools or the python library pyrokinetics. DREAM is a flux-surface averaged code, thus simulating only across the radial coordinate, but is able to include the effect of shaping. The elongation in particular has been found to reduce the generation of REs in previous studies [11] and the shaping is included in the simulations of sections 2 and 3. STEP flux surfaces are shown in Figure 1, as well as DREAM simulation domain. A conformal wall is also included, with a plasma-wall gap of $d_{wall} = 20\ cm$ and a wall time of $\tau_{wall} = 50\ ms$ for most of the simulations presented in this paper. Regarding runaway electron generation mechanisms, state-of-the-art fluid rates are used for Dreicer [12], hot-tail [13] and avalanche [12]. Tritium β decay and Compton scattering are not included in the modelling yet, but would further increase the primary RE generation in STEP active phase. While the temperature evolution

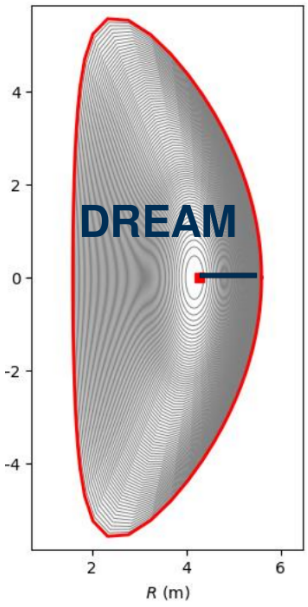

FIG. 1. STEP-EC-HD-v3 equilibrium and sketch of DREAM 1D radial domain (flux surface averaged).

will be self-consistent in the following sections, on mitigation, we start by modelling unmitigated disruptions with a prescribed temperature evolution, i.e. by specifying a thermal quench time (t_{TQ}) and a final electron temperature ($T_{e,final}$). Figure 2 shows the evolution of the total plasma current I_p, the Ohmic current I_{Ohm} and the runaway electron current I_{RE} for a prescribed TQ with $t_{TQ} = 3\ ms$ and $T_{e,final} = 10\ eV$. The prescribed TQ induces a current quench lasting $t_{CQ} \simeq 117\ ms$, during which a RE plateau with a RE current of $14.7\ MA$ is formed. The conversion rate between the initial plasma current and the final RE current (CR $= I_{RE,final}/I_{p,0}$)

is found to be 74 % in that particular case. Scans of the prescribed parameters have been performed for those unmitigated disruptions simulations, i.e. $t_{TQ}[ms] \in [0.6 - 10]$, $T_{e,final}[eV] \in [1 - 60]$, $d_{wall}[m] \in [0.1 - 0.5]$, $\tau_{wall}[ms] \in [10 - 500]$. Depending on those assumptions the final RE current can vary significantly, between 10 MA and full conversion ($I_{RE} \simeq 20\ MA$), with the shorter and colder TQ inducing the highest RE beam currents. Hot-tail is the dominant primary generation mechanism and the avalanche generation rate is orders of magnitude higher than all the other generation rates. Note that shaping is found to reduce the final RE current by about 10 % compared to the same case run in cylindrical geometry.

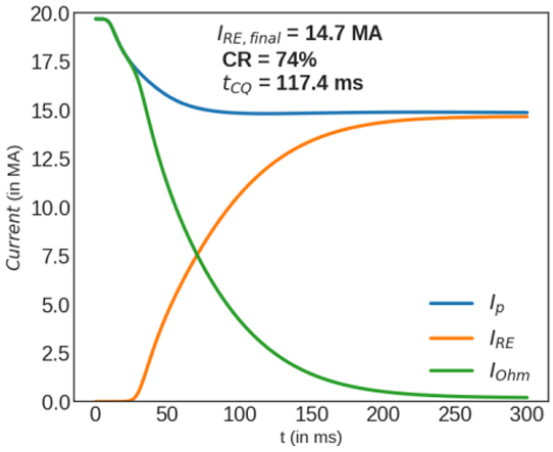

FIG. 2. Runaway electron generation in STEP-EC-HD-v3 unmitigated disruption with prescribed thermal quench ($t_{TQ} = 3\ ms$ and $T_{e,final} = 10\ eV$)

3. IDEALISED IMPURITY INJECTIONS

Disruption mitigation by idealised, i.e. radially uniform, impurity injection of a mixture of argon and D_2 was then modelled for STEP, with RE transport arising from the disruption of the magnetic flux surfaces (i.e. Rechester-Rosenbluth [14]). DREAM solves the energy balance equation given in [10], and the impurities are deposited uniformly in the plasma as in [5]. This impurity injection is clearly idealised, but is useful to find what core densities would be needed to prevent hot-tail generation of REs and reduce as much as possible the final RE current. Figure 3 shows an example of such a simulation: after a first simulation lasting 1 μs to initialise the profiles (see 3f for initial n_e and T_e) and get a self-consistent electric field, the impurities are added as a radially uniform neutral density. In that case, we have used $n_{Ar} = 5.10^{18}\ m^{-3}$, $n_{D_2} = 10^{21}\ m^{-3}$. The plasma is drastically diluted by the large quantities of deuterium injected (see central temperature in red on Figure 3a), and then argon radiates most of the thermal energy (see 3a and 3d). We also use an ad-hoc TQ thermal transport, to represent that caused by magnetic stochasticity, with normalised perturbation $\delta B/B = 2.10^{-3}$, which reduces the plasma temperature to about 1 eV. Note that in the TQ, both the Dreicer and the hot-tail generation are extremely small (more than 10 orders of magnitude smaller than the unmitigated cases in 2, see 3c) and the injection thus fulfills its purpose. The current quench then occurs (see 3a), increasing the parallel electric field to large values (3e shows the ratio of the parallel electric field with the effective critical electric field for RE generation, as derived in [15]). During the phase with high electric field, the RE population is quite small but grows through avalanche, before eventually forming a large population of runaway electrons (see the RE density on 3b) and a large 11.2 MA RE beam (see 3a).

Scanning the injected argon neutral density ($n_{Ar}[m^{-3}] \in [5.10^{17} - 10^{20}]$) and deuterium neutral density ($n_{D_2}[m^{-3}] \in [10^{20} - 10^{22}]$), we obtain a final RE current (at $t = 200\ ms$) between 15 MA and 8 MA, as shown in Figure 4. This is much higher than the LOCA (Loss of Coolant Accident) limit for ITER DMS of $I_{RE} = 0.5$ MA. While a similar limit is not yet well defined for STEP, such a RE beam will likely cause significant damage to PFCs and thus must be mitigated by additional systems. The smallest RE beams are achieved for relatively low densities of argon, which is not compatible with the DMS constraints on radiation fraction and on CQ time (Figure 4c and 4e). Too much argon and deuterium, as well as increasing I_{RE}, decreases the CQ time too much and increases the peak Heat Impact Factor (HIF) above the tungsten melt limit of 60 $MJ.m^2.s^{-0.5}$[16] (see Figure 4e and 4d). Figure 4f plots a normalised overlap parameter taking those constraints into account, to find optimal injection densities of $n_{Ar} \simeq 10^{18}\ m^{-3}$, $n_{D_2} \simeq 10^{21}\ m^{-3}$ (green star) which fulfill all non-RE DMS constraints (but with a RE beam current above 10 MA).

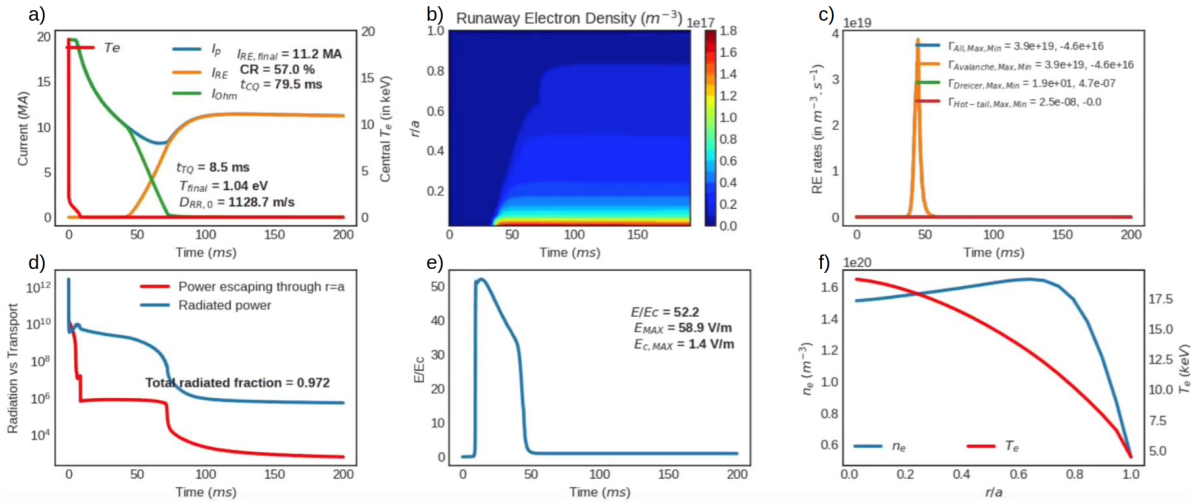

FIG. 3. Idealized impurity injection case using an Ar+D_2 mixture ($n_{Ar} = 5.10^{18}\ m^{-3}$, $n_{D_2} = 10^{21}\ m^{-3}$). Rechester-Rosenbluth transport with a magnetic perturbation of $\delta B/B = 2.10^{-3}$ is active during ionization and thermal quench phases. a) Central electron temperature evolution and total, ohmic and runaway currents. b) Evolution of the runaway electron density profile. c) Evolution of the integrated runaway electron generation rates. d) Evolution of the power escaping through the outer boundary and the integrated radiated power. e) Evolution of the parallel electric field divided by the effective critical electric field for runaway electron generation. f) Initial electron density and temperature profiles.

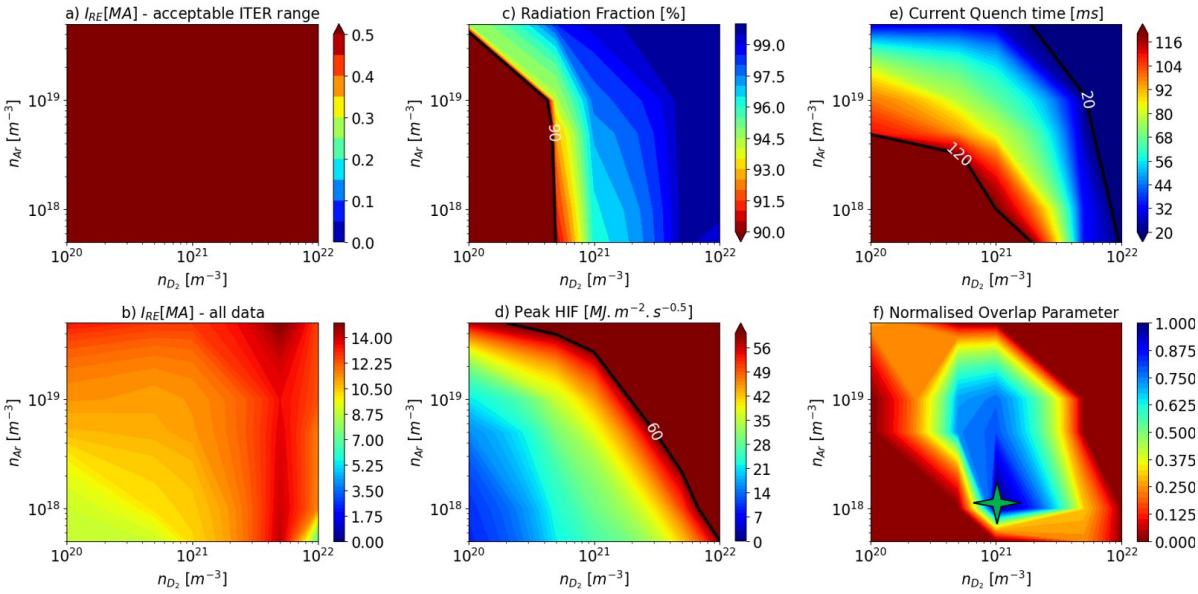

FIG. 4. Idealized impurity injection scan using an Ar+D_2 mixture. Rechester-Rosenbluth transport with a magnetic perturbation of $\delta B/B = 2.10^{-3}$ is active during ionization and thermal quench phases. a) and b) show the runaway current after 200 ms with different color bars (I_{RE} is above the limit in all cases); c) the total radiation fraction; d) the peak heat impact factor on the first wall during the radiation flash; e) the current quench time; For a),c),e) & d), everything which is out of the colorbar range does not fulfill the specific DMS constraint. f) shows the normalised overlap parameter which combines the DMS constraints (blue is good, red is bad, and the RE constraint is not fulfilled in any case).

Injections of a mixture of neon and D_2 have also been performed, showing a slightly lower generation of runaways, likely due to the lower number of bound electrons acting as a runaway source during avalanche. However, recent indications of argon being easier to purge for benign RE beam termination [17] and fuel cycle considerations in STEP (argon is already used for divertor seeding to control plasma detachment) promote the use of argon in STEP DMS.
Sustained particle loss in a stochastic magnetic field can reduce RE generation. This usually occurs naturally during disruption thermal quenches, but can also be driven during the current quench by using a passive Runaway Electron Mitigation Coil (REMC) or an equivalent conducting structure, one of which is planned for DIII-D and is the primary RE mitigation system in the SPARC tokamak [4]. Adding REMC-like transport during the current quench of the previous STEP simulations can greatly reduce the runaway generation, however only if the CQ $\delta B/B$, i.e. increased RE transport, is significant in the plasma core. This motivates a more detailed study to assess the viability of a REMC or an equivalent structure in STEP, i.e. including 3D non-linear MHD and 3D modelling of the conducting structures.

4. TESTING STEP DMS CONCEPT DESIGN USING DREAM SPI MODELLING

More realistic particle deposition profiles can substantially impact the results [3], and STEP DMS concept design needs to be optimized and tested in terms of pellet assimilation into the plasma. In particular, recent studies for ITER with the code INDEX [18] have shown that large pellets (such as planned for STEP) may not be fully assimilated by the target plasma. The DREAM SPI model has been benchmarked against INDEX (without plasmoid drifts) and JOREK, and is thus used to conduct a SPI DMS study for STEP. We model a two-stage SPI scheme as in ITER [3], with dilution cooling from pure D_2 pellets, followed by a strongly radiating phase due to mixed argon+D_2 pellets. We scan the injection parameters of the current STEP DMS concept design, which consists of 12 injectors of 22 mm pure D_2 pellets for Runaway Electron Avoidance (REA), 15 injectors of mixed Ar+D_2 16 mm pellets for TQ/CQ mitigation, and 30 injectors of pure D_2 7.5 mm pellets for Runaway Electron beam Mitigation (REM), all uniformly spaced at three different toroidal locations and multiple poloidal locations. The latter injectors cannot properly be studied in DREAM, due to the lack of MHD and molecular processes during the CQ phase (see [17]) so only the first two stages will be modelled. We define the number of shards to use in the simulation by solving the Statistical Fragmentation Model [19] during DREAM input file creation. In some cases, the number of shards needs to be reduced for the simulation to run, but as will be discussed in section 5 this has a small impact on the results.
Figure 5 shows such a simulation, with a subset of the 12x15 SPIs launched from the conformal wall, and the typical evolution of the electron temperature and the runaway electron density. The first SPI injection of pure D_2 starts after 3 ms ($v_{inj,\ D\ SPI} = 400\ m.s^{-1}$) and dilutes the plasma drastically, increasing the plasma density and decreasing the electron temperature to $\simeq 100\ eV$. Compared to unmitigated disruptions shown in section 2, the hot-tail generation of REs is greatly reduced. However, both hot-tail and Dreicer generation are much higher than for the idealised impurity injections shown in the previous section. Then, the second SPI starts at 7 ms ($v_{inj,\ Ar\ SPI} = 200\ m.s^{-1}$) and radiates almost all the plasma thermal energy. During that phase, we activate an ad-hoc ¨MHD¨ TQ when the shards reach the q = 3 surface (by design, there is no q = 2 surface in STEP plasmas), lasting 1 ms (as in [20]) and with a $\delta B/B = 2.10^{-3}$. The impact of that choice will be discussed in section 5. Both the argon line radiation and the thermal transport due to ¨MHD¨ decreases the electron temperature to a few eV post-TQ, as can be seen on Figure 6. Unfortunately, both Figure 5 and 6 show the generation of a large RE beam carrying 12.7 MA of current.
Interestingly, the simulation results (i.e. the final RE current) are quite insensitive to the number of injectors used in the simulations. Studying the evolution of the pellet shards in the full simulations (see cyan dots in Figure 5 as a example) shows that the pellet shards are not fully assimilated even for the lowest injection quantities of STEP DMS concept design (i.e. 1 injection of a pure 22 mm D_2 pellet, followed by 1 injection of a 16 mm $Ar + D_2$ pellet, when the maximum that can be injected is 12x15 injectors). Simulations with a scaled-down DMS system show that we can reach full assimilation of the pellets, but we also obtain 12.5 MA of RE current for those cases. When further reducing the injected argon quantities, we don't have a current quench anymore, while reducing the first SPI D_2 quantities increases the final I_{RE} (higher hot-tail generation) up to 14.5 MA.

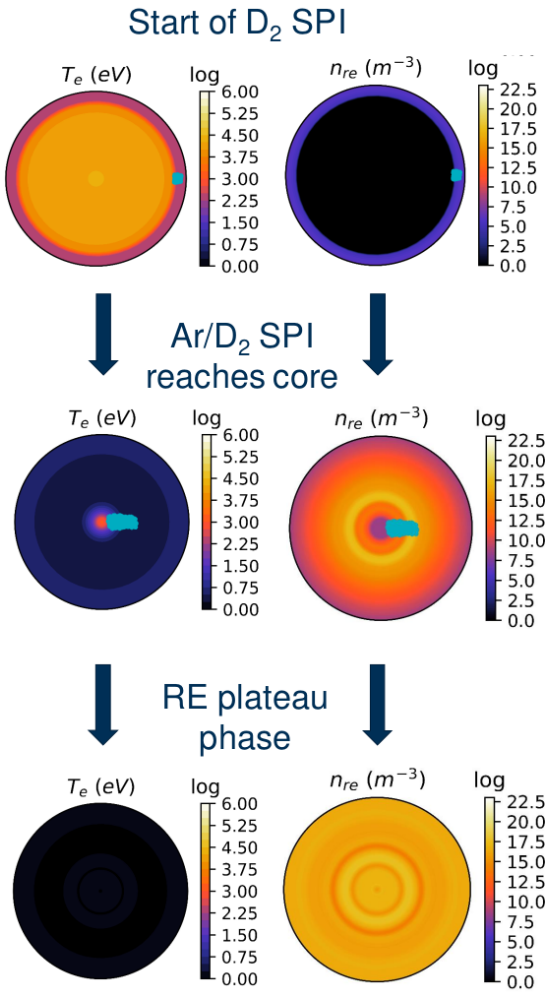

FIG. 5. 2D representation of DREAM 1D modelling of 2-stage SPI injection into STEP-EC-HD-v3, with $N_D = 2.10^{23}$ atoms, $N_{Ar} = 4.10^{21}$ atoms. The evolution of the cold electron temperature, T_e, is shown on the left and the evolution of the runaway electron density, n_{re}, on the right.

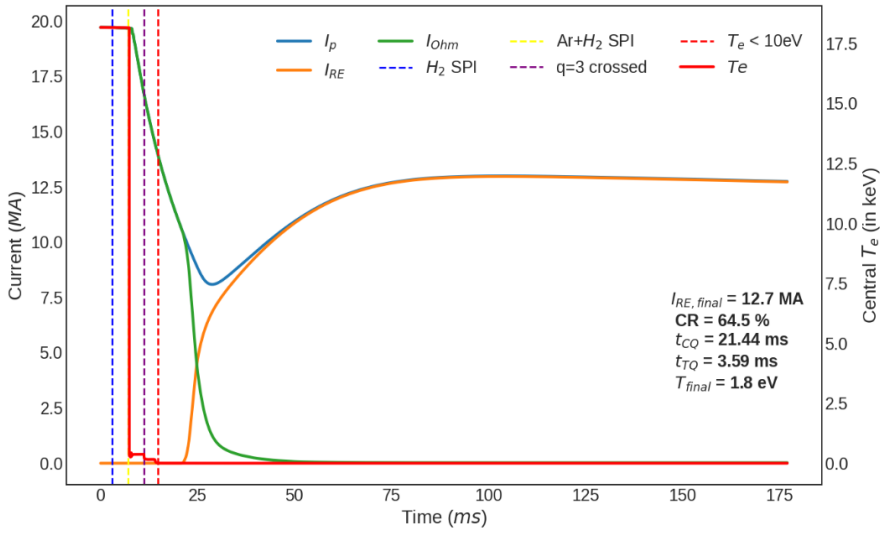

FIG. 6. 2-stage SPI injection into STEP-EC-HD-v3, with $N_D = 2.10^{23}$ atoms, $N_{Ar} = 4.10^{21}$ atoms. Vertical dash lines indicate the start of the D_2 SPI (blue), the start of the $Ar + D_2$ SPI (yellow), when the 2nd SPI shards cross the q = 3 surface (purple) and when the core temperature goes below $10\ eV$ (red). The evolution of the total plasma current I_p, the ohmic current I_{Ohm} and the RE current I_{RE} is also shown.

5. DISCUSSION & CONCLUSIONS

The impact of the modelling assumptions on the results presented in section 4 have been explored. Some have a minor effect, such as the number of pellet shards (at constant injected atoms), increasing the 1D radial resolution or having smaller time steps. Recent work has also shown that the Dreicer and Hot-tail generation rates in DREAM fluid model could be overestimated for plasmas with low-Z (as the model was derived for high-Z). We have thus run a few STEP cases limiting the hot-tail generation (by two orders of magnitude). While preliminary, this study so far shows that the final RE current is barely affected. To better model the hot-tail generation, a few cases have also been run with DREAM isotropic model [10] (only for idealised impurity injections), which show a slight reduction of the final RE current, so future SPI cases should be done using DREAM isotropic (or super-thermal) models, to assess the validity of the fluid results.
Other parameters have however a more significant effect, such as the addition of Tritium in the simulations. This has only been tested on a few cases, but is found to increase the final RE current by up to 3 MA (i.e. 15.5 MA instead of 12.5 MA) for a 50/50 D-T mixture, through the additional RE source from Tritium β decay. While not included so far as the total photon gamma flux has not yet been modelled in STEP, Compton scattering is likely to increase I_{RE} even further during STEP active phase (as shown in [3] for ITER).
Sensitivity scans on the TQ $\delta B/B$ choice (both amplitude and duration) have shown it can have a very large effect on the results. The cases presented in section 4 used a radially uniform $\delta B/B = 2.10^{-3}$, applied for 1 ms, and obtained a 12.7 MA RE beam. Compared to those, decreasing $\delta B/B$ increases I_{RE} progressively, up to 16.6 MA for $\delta B/B = 1.10^{-4}$ (still applied for 1 ms). Increasing $\delta B/B$ higher than 2.10^{-3} however does not decrease I_{RE} substantially. Keeping $\delta B/B = 2.10^{-3}$ but varying the ¨MHD¨ TQ duration also changes the final I_{RE} (9 MA for 15 ms, 16 MA for 0.1 ms). This highlights the importance of performing high-fidelity 3D non-linear MHD modelling of STEP mitigated disruptions in order to constrain and justify the choice of RE transport parameters in DREAM (as was done for SPARC [4] or ITER [21], for example).
Finally, the simulations did not include the effect of plasmoid drifts. In STEP, the REA SPI are planned on the HFS of the device and thus we would expect a beneficial effect of the plasmoid drifts on the core assimilation of those pellets. A model to account for this, based on [22], has very recently been implemented in DREAM. The effect it has on the results presented in this paper will be studied next.

In conclusion, STEP DMS performance regarding RE generation and avoidance has been studied, and 2-stage SPI injections are found to reduce hot-tail generation. However, this is not enough to avoid the formation of a large $\geq$ 10 MA RE beam. To tackle this issue, the STEP concept design currently includes 30 D_2 SPI (with MGI as another option) systems dedicated to RE beam mitigation. This includes redundancy and assumes repetitive injections during the RE plateau to keep the neutral pressure high enough to expect a ¨benign¨ termination of the RE beam [23]. While very preliminary, recent investigations using the 1D neutral diffusion model of [17] have shown that STEP mitigated disruptions could be in such a regime with the need of only a limited amount of CQ injections. While the potential of such a scheme has been demonstrated on existing fusion devices such as JET [24], further extensive modelling of STEP using 3D non-linear MHD codes such as JOREK [25] is essential and very high priority for the STEP programme. Experimental results from ITER and SPARC will also be essential to validate and optimise STEP DMS. Finally, passive and/or active 3D fields induced during the CQ could also reduce substantially RE generation, and must be assessed urgently.

REFERENCES

[1] M. Lehnen et al. “Disruptions in ITER and strategies for their control and mitigation”. In: *Journal of Nuclear Materials* 463 (Aug. 2015), pp. 39–48. DOI: 10.1016/j.jnucmat.2014.10.075.

[2] H Meyer. “The plasma scenarios for the spherical tokamak for energy production (STEP) and their technical implications”. In: *this conference* (2023).

[3] Oskar Vallhagen et al. “Effect of two-stage shattered pellet injection on tokamak disruptions”. In: *Nuclear Fusion* (2022). DOI: 10.1088/1741-4326/ac667e.

[4] Roy Alexander Tinguely et al. “Modeling the complete prevention of disruption-generated runaway electron beam formation with a passive 3D coil in SPARC”. In: *Nuclear Fusion* (2021). DOI: 10.1088/1741-4326/ac31d7.

[5] Esmée Berger et al. “Runaway dynamics in reactor-scale spherical tokamak disruptions”. In: *Journal of Plasma Physics* 88.6 (Dec. 2022), p. 905880611. DOI: 10.1017/S0022377822001209.

[6] V. A. Izzo et al. “Runaway electron deconfinement in SPARC and DIII-D by a passive 3D coil”. In: *Nuclear Fusion* 62.9 (Aug. 2022), p. 096029. DOI: 10.1088/1741-4326/ac83d8.

[7] Yueqiang Liu et al. "Toroidal modeling of runaway electron loss due to 3-D fields in ITER". In: *Nuclear Fusion* (2022). DOI: 10.1088/1741-4326/ac5d62.

[8] V Bandaru et al. "Magnetohydrodynamic simulations of runaway electron beam termination in JET". In: *Plasma Physics and Controlled Fusion* 63.3 (Mar. 2021), p. 035024. DOI: 10.1088/1361-6587/abdbcf.

[9] Chang Liu et al. "Self-consistent simulation of resistive kink instabilities with runaway electrons". In: *Plasma Physics and Controlled Fusion* 63.12 (Nov. 2021), p. 125031. DOI: 10.1088/1361-6587/ac2af8.

[10] Mathias Hoppe, Ola Embreus, and Tünde Fülöp. "DREAM: A fluid-kinetic framework for tokamak disruption runaway electron simulations". In: *Computer Physics Communications* 268 (Nov. 2021), p. 108098. DOI: 10.1016/j.cpc.2021.108098.

[11] T. Fülöp et al. "Effect of plasma elongation on current dynamics during tokamak disruptions". In: *Journal of Plasma Physics* 86.1 (Feb. 2020), p. 474860101. DOI: 10.1017/S002237782000001X.

[12] L. Hesslow et al. "Evaluation of the Dreicer runaway generation rate in the presence of high-impurities using a neural network". In: *Journal of Plasma Physics* 85.6 (Dec. 2019), p. 475850601. DOI: 10.1017/S0022377819000874.

[13] Ida Svenningsson et al. "Hot-Tail Runaway Seed Landscape during the Thermal Quench in Tokamaks". In: *Physical Review Letters* 127.3 (July 14, 2021), p. 035001. DOI: 10.1103/PhysRevLett.127.035001.

[14] A. B. Rechester and M. N. Rosenbluth. "Electron Heat Transport in a Tokamak with Destroyed Magnetic Surfaces". In: *Physical Review Letters* 40.1 (Jan. 1978), pp. 38–41. DOI: 10.1103/PhysRevLett.40.38.

[15] L. Hesslow et al. "Effect of partially ionized impurities and radiation on the effective critical electric field for runaway generation". In: *Plasma Physics and Controlled Fusion* 60.7 (June 2018), p. 074010. DOI: 10.1088/1361-6587/aac33e.

[16] M Sugihara et al. "Disruption scenarios, their mitigation and operation window in ITER". In: *Nuclear Fusion* 47.4 (Apr. 2007), pp. 337–352. DOI: 10.1088/0029-5515/47/4/012.

[17] E. M. Hollmann et al. "Trends in runaway electron plateau partial recombination by massive H2 or D2 injection in DIII-D and JET and first extrapolations to ITER and SPARC". In: *Nuclear Fusion* 63.3 (Feb. 2023), p. 036011. DOI: 10.1088/1741-4326/acb4aa.

[18] A. Matsuyama et al. "Enhanced Material Assimilation in a Toroidal Plasma Using Mixed H+Ne Pellet Injection and Implications to ITER". In: *Physical Review Letters* 129.25 (Dec. 14, 2022), p. 255001. DOI: 10.1103/PhysRevLett.129.255001.

[19] T. E. Gebhart, L. R. Baylor, and S. J. Meitner. "Shatter Thresholds and Fragment Size Distributions of Deuterium–Neon Mixture Cryogenic Pellets for Tokamak Thermal Mitigation". In: *Fusion Science and Technology* 76.7 (Oct. 2020), pp. 831–835. DOI: 10.1080/15361055.2020.1812991.

[20] D. Hu et al. "Radiation asymmetry and MHD destabilization during the thermal quench after impurity shattered pellet injection". In: *Nuclear Fusion* 61.2 (Jan. 2021), p. 026015. DOI: 10.1088/1741-4326/abcbcb.

[21] Di Hu et al. "Collisional-radiative simulation of impurity assimilation, radiative collapse and MHD dynamics after ITER Shattered Pellet Injection". In: *Nuclear Fusion* (Mar. 2023). DOI: 10.1088/1741-4326/acc8e9.

[22] O. Vallhagen et al. "Drift of ablated material after pellet injection in a tokamak". In: *Journal of Plasma Physics* 89.3 (June 2023), p. 905890306. DOI: 10.1017/S0022377823000466.

[23] C. Paz-Soldan et al. "A novel path to runaway electron mitigation via deuterium injection and current-driven MHD instability". In: *Nuclear Fusion* 61.11 (Oct. 2021), p. 116058. DOI: 10.1088/1741-4326/ac2a69.

[24] C. Reux et al. "Physics of runaway electrons with shattered pellet injection at JET". In: *Plasma Physics and Controlled Fusion* 64.3 (Feb. 2022), p. 034002. DOI: 10.1088/1361-6587/ac48bc.

[25] Matthias Hoelzl et al. "The JOREK non-linear extended MHD code and applications to large-scale instabilities and their control in magnetically confined fusion plasmas". In: *Nuclear Fusion* (Apr. 2021). DOI: 10.1088/1741-4326/abf99f.